JOURNAL OF GEOPHYSICAL RESEARCH, VOL. 113, A02205, doi:10.1029/2007JA012456, 2008

Two classes of earthward fast flows in the plasma sheet

J.-H. Shue,[1] A. Ieda,[2] A. T. Y. Lui,[3] G. K. Parks,[4] T. Mukai,[5] and S. Ohtani[3]

Received 9 April 2007; revised 8 October 2007; accepted 10 October 2007; published 7 February 2008.

[1] In this study we first identify earthward plasma sheet fast flows from Geotail plasma and magnetic fields with a criterion of $V_{\perp x} > 300$ km/s, where $V_{\perp x}$ is the X component of the plasma flow perpendicular to the ambient magnetic field. We then estimate rates of change of the nightside auroral power over the courses of the fast flows using Polar Ultraviolet Imager auroral images. It is found that 68 earthward fast flows observed at $|Y| < 6\ R_E$ during 1997–1998 can be classified into two classes. One class of the earthward fast flows (Class *I*) was often observed near $X = \sim -10\ R_E$ and the other class (Class *II*) was found at $X < -15\ R_E$. The auroral power rates of change of the fast flows in Class *I* in terms of time are found to be high, indicating that the total auroral power on the nightside was significantly increasing during these fast flows. The corresponding auroral images show an apparent substorm bulge developed on the nightside, i.e., a significant global auroral development. The auroral power rates for most of the earthward fast flows in Class *II* are low. The auroral features, such as poleward boundary intensifications and pseudobreakups, are found to be associated with these fast flows. Some of the earthward fast flows in Class *II* can propagate earthward and provide a favorable condition for a substorm onset, leading to an auroral bulge developed on the nightside. We have also tested another criterion of $V_xB_z > 2$ mV/m for an identification of fast flows, where V_x is the X component of the plasma flow and B_z is the Z component of the geomagnetic field. It is found that $V_{\perp x}$ is a better parameter than V_xB_z to differentiate the two classes of earthward fast flows in the plasma sheet.

Citation: Shue, J.-H., A. Ieda, A. T. Y. Lui, G. K. Parks, T. Mukai, and S. Ohtani (2008), Two classes of earthward fast flows in the plasma sheet, *J. Geophys. Res.*, *113*, A02205, doi:10.1029/2007JA012456.

1. Introduction

[2] The properties of plasma and magnetic fields in the near-Earth region vary in response to changing solar wind conditions and the state of the magnetosphere. The magnetotail is stretching and the magnetospheric convection is enhancing when the interplanetary magnetic field is southward. The magnetospheric configuration becomes dipolarized after a substorm expansion onset occurs. The energy stored in the magnetotail is then suddenly released into the high-latitude ionosphere, causing an auroral bulge on the nightside. This auroral bulge is commonly considered as the main auroral feature for a substorm. For some cases, a substorm cannot develop to a full-scale one. The auroral brightness lasts only a few minutes and dies down, or brightens intermittently. These auroras are usually called pseudobreakups [*Akasofu*, 1964] or small substorms. The main feature of a pseudobreakup displayed in global auroral images is a bright spot. The poleward boundary intensification (PBI) is another type of aurora, mainly occurring at the poleward edge of the auroral oval in the premidnight sector. The PBI can occur at all phases of substorms [*Lyons et al.*, 1999].

[3] The speed of plasma flows in the plasma sheet is normally slow [*Huang and Frank*, 1986; *Baumjohann et al.*, 1988, 1989]. In some occasions, the plasma flows may exceed 400 km/s [*Baumjohann et al.*, 1990; *Angelopoulos et al.*, 1992]. Several physical mechanisms can interpret the generation of fast flows in the plasma sheet. *Nagai et al.* [1998] and *Machida et al.* [1999] used the near-Earth magnetic reconnection [*Hones*, 1976] to interpret the earthward fast flows with the northward geomagnetic fields and the tailward fast flows with the southward geomagnetic fields observed at 20–30 R_E down the tail. Through the magnetic reconnection mechanism, the energy of the magnetic fields is converted to the kinetic energy, i.e., the plasma is accelerated to the high speed. *Lui et al.* [1993] proposed a force imbalance caused by the current disruption mechanism to interpret the earthward fast flows observed near $X = \sim -10\ R_E$. The generation of the earthward fast flows can be also interpreted by the plasma

[1]Institute of Space Science and Department of Atmospheric Sciences, National Central University, Jhongli, Taiwan.
[2]Solar-Terrestrial Environment Laboratory, Nagoya University, Nagoya, Aichi, Japan.
[3]Applied Physics Laboratory, Johns Hopkins University, Laurel, Maryland, USA.
[4]Space Sciences Laboratory, University of California, Berkeley, California, USA.
[5]Institute of Space and Astronautical Science, Japan Aerospace Exploration Agency, Sagamihara, Kanagawa, Japan.

0148-0227/08/2007JA012456$09.00

bubble mechanism [*Chen and Wolf*, 1993]. A localized bubble originated in the distant tail moves earthward at high speed owing to the polarization electric fields in the bubble. In addition, the magnetic reconnection in the distant tail [*Nagai and Machida*, 1998], a retreat of the tailward fast flows generated by a near-Earth neutral line [*Baumjohann et al.*, 1999], and an enhancement of large-scale ultra-low frequency waves in the magnetosphere [*Lyons et al.*, 2002] are the possible mechanisms for the generation of earthward fast flows.

[4] The fast flows, in nature, are transient [*Baumjohann et al.*, 1990; *Angelopoulos et al.*, 1992; *Ohtani et al.*, 2004] and spatially localized [*Angelopoulos et al.*, 1997; *Slavin et al.*, 1997]. The occurrence rates of the fast flows for disturbed times are larger than those for quiet times [*Angelopoulos et al.*, 1994]. The earthward fast flows are believed to play an important role in the magnetic flux transport [*Angelopoulos et al.*, 1992, 1994, 1999; *Miyashita et al.*, 2003].

[5] Relationships between plasma sheet fast flows and auroras were studied by using Geotail plasma and magnetic fields, and Polar Ultraviolet Imager (UVI) auroral images after the Polar satellite was launched. *Lui et al.* [1998] first identified substorm auroral breakups using the Polar UVI images, and then examined the Geotail data for the existence of fast flows in association with the auroral breakups. They found that the fast flows were not always present during the periods of the substorm breakups. *Ieda et al.* [2003] first searched for quiet intervals using the Polar UVI images, and then examined the existence of fast flows. The fast flows were rarely found in the quiet intervals identified in their study.

[6] The relationships between plasma sheet fast flows and auroras were also studied in an opposite way, i.e., first identifying fast flows, and then examining their associated electrojets or auroral activities. *Fairfield et al.* [1999] found that auroral brightenings developed near the foot point of Geotail where the earthward fast flows were observed in the magnetotail. *Nakamura et al.* [2001] concluded that all the earthward fast flows were associated with the localized auroral activations such as pseudobreakups or PBIs. The localized auroral activations can be explained by a current wedge created by a shear at the outer edge of a fast flow [*Birn and Hesse*, 1996]. It should be noted that *Nakamura et al.* [2001] did not include the events of full-developed substorms in their data set. Thus their conclusion is valid only for the weak auroral activations. *Shue et al.* [2003] found that half of the earthward fast flows are associated with decreasing auroral power integrated over a nightside region using Polar UVI auroral images. They also found some earthward fast flows occurred during the periods of no auroral activations. It is interpreted that the earthward fast flows can create a favorable condition for a development of a substorm expansion onset [*Ohtani et al.*, 2002], implying that the earthward fast flows may not have a direct contribution to the substorm aurora. *Shay et al.* [2003] used a 3-D two-fluid code to simulate the magnetic reconnection, which is a mechanism for the generation of fast flows. They concluded that the thickness of the initial current sheet in the magnetotail may ultimately determine the scale size (localized or global) of the magnetic reconnection.

[7] It is still under debate whether the earthward fast flows are associated with the auroral brightening and further development. Some previous studies [e.g., *Angelopoulos et al.*, 1992, 1994, 1999; *Miyashita et al.*, 2003] positively support the statement, but some claim or imply a lack of supports [e.g., *Paterson et al.*, 1998; *Lui et al.*, 1999; *Nakamura et al.*, 2001; *Ohtani et al.*, 2002]. In particular, *Lui et al.* [1999] showed that near-Earth dipolarization can occur without any significant flows preceded. From these studies, there seems to have a tendency of two classes of the earthward fast flows. One class is associated with the global auroral development and the other is associated with the localized auroral activations. To our knowledge, no research has been performed to systematically investigate the two classes of the earthward fast flows in the same study. In addition, we have investigated the dependence of the earthward fast flows on X in the GSM coordinate system and their associated auroral features in the noon-midnight meridian.

2. Data Reduction

[8] In this study we use the 12-s average low energy particle (LEP) data [*Mukai et al.*, 1994] and magnetic field (MGF) data [*Kokubun et al.*, 1994] to identify earthward fast flows in the plasma sheet. We also use the Polar UVI auroral images at the Lyman-Birge-Hopfield long band (~170.0 nm) [*Torr et al.*, 1995] to determine the auroral features associated with the fast flows. Two years of the Geotail data and Polar images (1997–1998) were surveyed.

[9] We define an earthward fast flow as $V_{\perp x} > 300$ km/s, where $V_{\perp}x$ is the X component of the plasma flow perpendicular to the ambient magnetic field. The blue horizontal line on the $V_{\perp x}$ panel in Figure 1a denotes the threshold of 300 km/s for fast flows. The starting time of an event is designated as the time of the first data point with $V_{\perp x} > 300$ km/s. Since Geotail was not always residing in the plasma sheet, we imposed a criterion of $\beta > 0.5$ on the Geotail plasma and magnetic fields [*Baumjohann et al.*, 1990; *Angelopoulos et al.*, 1994; *Ohtani et al.*, 2004] to find the region of the plasma sheet, where β is the ratio of the plasma pressure to the magnetic pressure. The threshold of β is marked by the blue horizontal line on the β panel in Figure 1a. We also used the criterion of $|Y| < 6\ R_E$ for choosing the events near the noon-midnight meridian.

[10] The interval for each event is 30 min, starting from 15 min before to 15 min after the starting time of the fast flows. Since the time resolution of Polar UVI images is ~3 min, it should have eleven images in the 30-min interval for each event. If the number of corresponding images for an event is less than nine images, we discard the event. Six Polar UVI auroral images have been plotted to show the auroral development for each event, see Figure 1b.

[11] The auroral power is estimated over a region of 60–80° MLAT and 2000–0400 MLT for each UVI image. We fit a straight line to all the available auroral power with a least squares method for each event. The slope of the line, as plotted in red in Figure 1c, is interpreted as the auroral power rate of change. A distribution of the 68 earthward fast flows in terms of the locations in the X-Y plane of the GSM coordinates is plotted in Figure 2. More events are found at $X < -15\ R_E$ than at $X > -15\ R_E$. Lacks of events in the

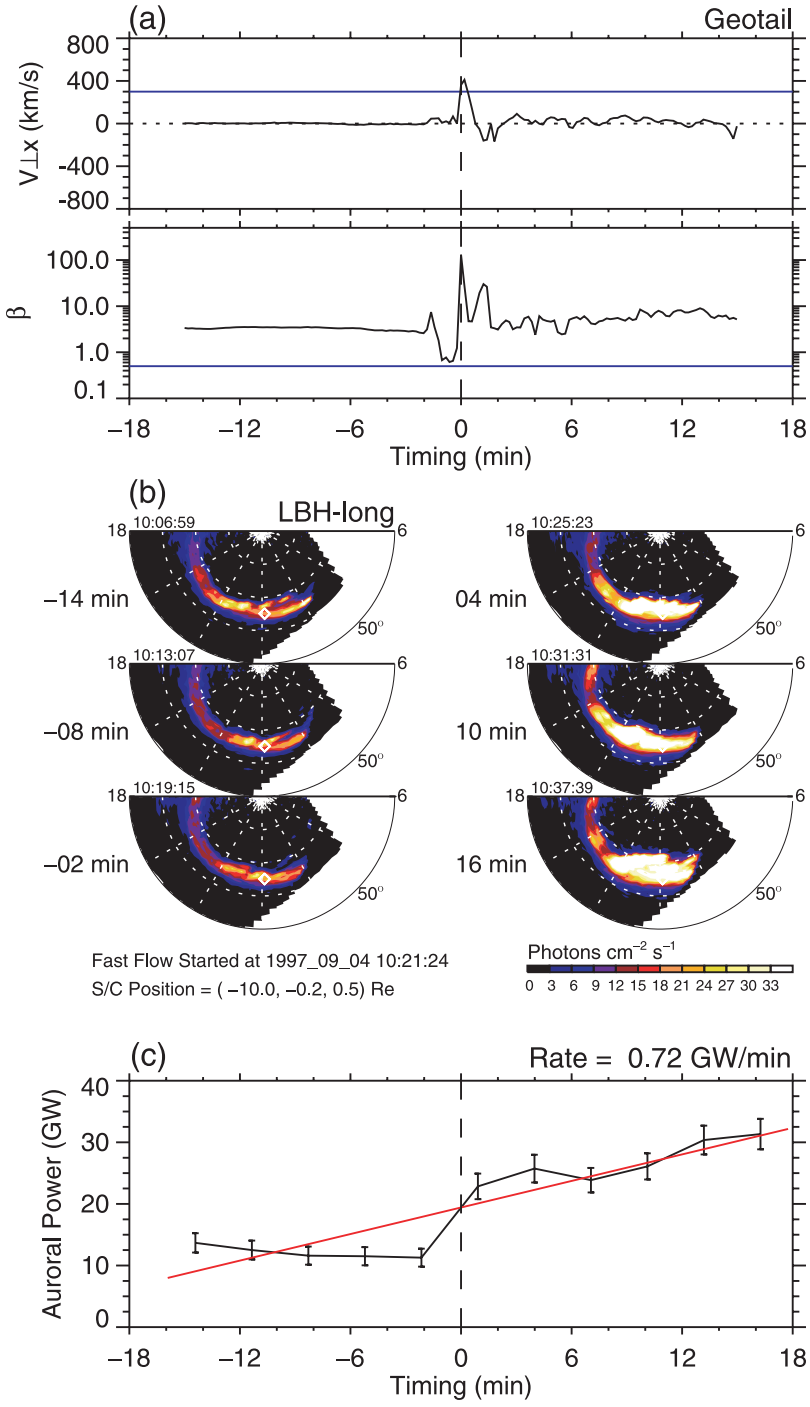

Figure 1. Observations of Geotail plasma and magnetic fields and Polar Ultraviolet Imager (UVI) auroral images for the 4 September 1997 event. (a) Geotail data have been shifted to the starting time of the fast flows, as marked by the vertical dash line. (b) The timings of Polar UVI auroral images have been shifted to the starting time of the fast flows. Negative (positive) timings marked on the left of the auroral images denote the time of the images taken before (after) the fast flow occurred. (c) Integrated auroral power is plotted against timing. A vertical bar on the auroral power indicates the uncertainty of the mean auroral power. The data points for the mean auroral power are fitted to a red line by a linear least squares method. The slope of the line is marked on the top.

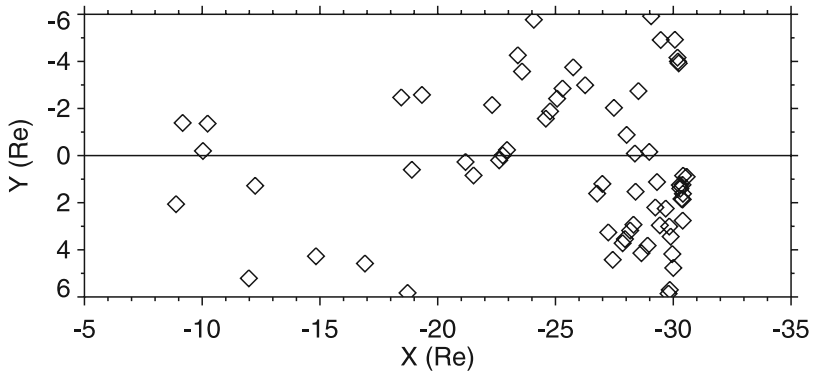

Figure 2. A distribution of the earthward fast flows in the X-Y plane in the GSM coordinate system. Diamonds denote the locations where Geotail observed the earthward fast flows ($V_{\perp x} > 300$ km/s).

premidnight at -19 to -26 R_E region and the postmidnight at -11 to -18 R_E region are mainly due to the unavailability of the corresponding Polar UVI auroral images to the events.

[12] The data sets and the selection criteria used in this study are the same as those of *Shue et al.* [2003]. For more information on the processing of the data sets and the selection criteria, the readers are referred to *Shue et al.* [2003].

3. Results

[13] We have identified 68 earthward fast flow events during which Geotail was located at the region of $|Y| < 6$ R_E down the tail and Polar had the corresponding auroral images to the events. The occurrence rates of the earthward fast flows have been normalized by the total observation time of Geotail spent at the region with the availability of the Polar auroral images. These occurrence rates have been plotted in terms of X in the GSM coordinate system in Figure 3. The occurrence rates are, in general, decreasing as Geotail comes closer to the Earth. However, the occurrence rate for $X = -10$ R_E is almost the same as that for $X = -15$ R_E. The uncertainty, marked as a vertical bar, is estimated from the square root of the number divided by the total observation time for each bin [*Shiokawa et al.*, 1997]. Although the occurrence rate from $X = -15$ R_E to $X = -10$ R_E has almost no change, we believe that there is some physical meaning in it when we consider the factor of the higher magnetic field pressure, which can slow down the speed of the fast flows, as the earthward fast flows come closer to the Earth. Under these circumstances, the occurrence rate at $X = -10$ R_E is supposed to be much smaller than what it has now been shown if there is no additional mechanism that generates earthward fast flows at $X = \sim -10$ R_E. This discussion is also supported by Figure 1a of *Shiokawa et al.* [1997], which shows that the occurrence rate of high-speed bulk flows for $X = -10$ R_E is higher than that for $X = -15$ R_E.

[14] In Figure 4, the auroral power rate has been plotted against X for all the 68 earthward fast flow events. The distribution of the auroral power rate can be divided into two classes. The fast flows in the first class (Class *I*) are found to be located at $X > -15$ R_E. The auroral power rates for all the events in Class *I* are high. However, the earthward fast flows in Class *II* are found to be located at $X < -15$ R_E. The auroral power rates for most of the events in Class *II* are low, but a few of them are high.

[15] We will show one earthward fast flow event in Class *I* and three earthward fast flow events in Class *II* for a demonstration of relationships between the auroral features and fast flows.

3.1. Earthward Fast Flow Event in Class *I*

[16] Figure 1 shows Geotail plasma and magnetic fields and Polar UVI auroral images for an event of the earthward fast flow in Class *I* for 4 September 1997. Geotail, which was located at $X = -10.0$ R_E, observed an earthward fast flow at 1021:24 UT. Geotail data have been shifted to the starting time of the fast flow in which the zero timing is designated. Positive (Negative) timings denote after (before) the fast flow occurred. The values of β were greater than 0.5

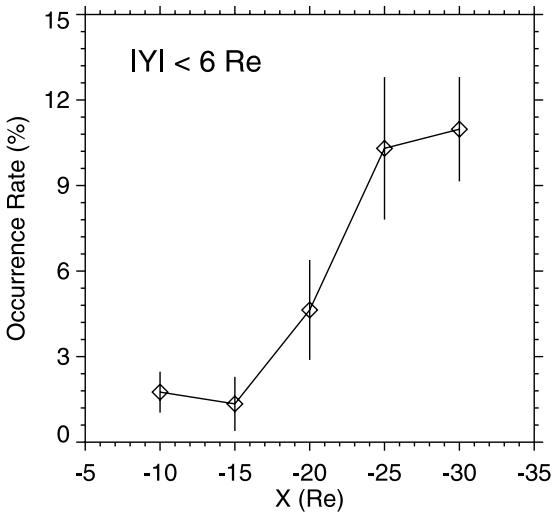

Figure 3. Occurrence rates of the earthward fast flows in terms of X in the GSM coordinate system. The occurrence rates have been normalized by the total observation time of Geotail at $|Y| < 6$ R_E down the tail with the availability of Polar UVI auroral images. The uncertainty, marked as a vertical bar, is estimated from the square root of the number divided by the total observation time for each bin. The change of the occurrence rates is consistent with that shown in Figure 1a of *Shiokawa et al.* [1997].

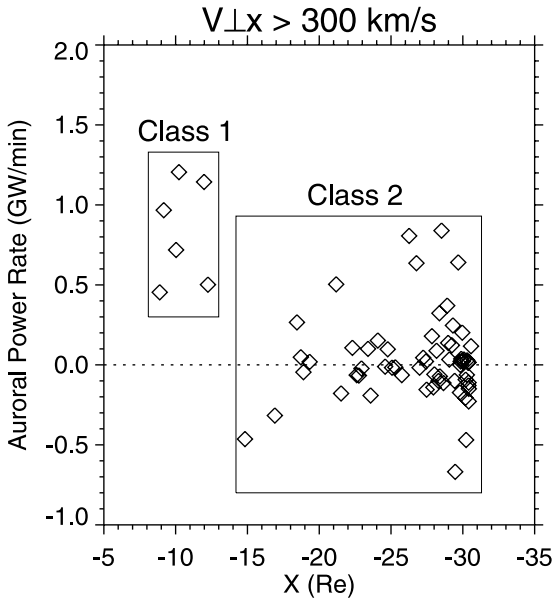

Figure 4. Auroral power rates of change estimated over the courses of earthward fast flows ($V_{\perp x}$ > 300 km/s) in terms of X in the GSM coordinate system. The auroral power is integrated over a region of 60–80° MLAT and 2000–0400 MLT.

during the event, indicating that Geotail was in the plasma sheet.

[17] Polar UVI auroral images taken during this fast flow event are shown in Figure 1b. Some auroral activities on the nightside occurred before the onset time of the fast flow. We used the *Tsyganenko* [1989] magnetospheric model to map the foot point of Geotail, as marked by the diamond on each image. It should be noted that the accuracy of the mapping of the foot point of Geotail depends upon the accuracy of a magnetospheric model. Moreover, a spot on the pre-existing aurora at premidnight began to brighten at the starting time of the fast flow (not shown) and continued developing to an auroral bulge. The foot point of Geotail was located at postmidnight.

[18] We estimated auroral power for each of the 11 images taken during the event. The auroral power has been plotted against timing in Figure 1c. There was a significant increase in the auroral power, from ~12 to 22 Gigawatts (GW), near the starting time of the earthward fast flow. We also estimated the uncertainty for the auroral power, as marked as the vertical bar on each data point of the auroral power. We fit a straight line to these data points by using a least squares method. The slope of the fitted line is 0.72 GW/min.

[19] For all the events in Class *I*, an auroral bulge always appears on the nightside, which results in a large auroral power rate, i.e., high auroral energy into the ionosphere.

3.2. Earthward Fast Flow Events in Class *II*

[20] Figure 5 shows Geotail plasma and magnetic field and Polar UVI auroral images for an event of the earthward fast flow in Class *II* for 21 November 1997. Geotail observed a fast flow at 1843:50 UT, as shown in Figure 5a. Geotail was located at $X = -19.3\ R_E$. The local magnetic fields were northward (not shown) and the values of β were >0.5 during the event. The foot point of Geotail was located at postmidnight.

[21] The auroral activity was weak before the fast flow occurred, as shown in Figure 5b. A small auroral spot, which is usually called a pseudobreakup, appeared near the foot point of Geotail at the zero timing. The auroral spot lasted ~6 min, and then faded its intensity to the background value. Figure 5c shows that the integrated auroral power increases slightly at the starting time of the fast flow. The auroral power rate for this event is 0.02 GW/min. This event clearly shows an association of an earthward fast flow with a localized auroral activation of pseudobreakups near the foot point of Geotail.

[22] Geotail observed a series of fast flows at X = -18.9 R_E, starting from 2148:48 UT during the 26 November 1997 event, as shown in Figure 6a. The local magnetic fields were northward (not shown) and the values of β were >0.5 during the event. The foot point of Geotail was located at premidnight. Figure 6b shows that a PBI had already been activated at -16 min at premidnight before the fast flows occurred. Its intensity was then decreasing until the fast flows occurred. The intensity of the PBI increased again and started decreasing 6 min later. The increase in the intensity of the PBI was reflected in the increase in the auroral power, as shown in Figure 6c. This event clearly shows an association of the earthward fast flows with a localized auroral activation of the PBI.

[23] In Class *II*, most of the events are associated with low auroral power rates. However, a few of them are associated with high auroral power rates. Figure 7 shows one example of such events in which the auroral power rate is high. Figure 7a shows that the fast flows, which were detected by Geotail at $X = -28.5\ R_E$, began at 1411:54 UT, 29 January 1997. The high auroral power rate for this event is due to an appearance of the auroral bulge at premidnight at −4 min before the fast flows occurred, as shown in Figure 7b. The resulting auroral power rate marked in Figure 7c is 0.84 GW/min. Interestingly, a pseudobreakup occurred at postmidnight near the foot point of Geotail. Thus the earthward fast flow observed at postmidnight is most likely related to the pseudobreakup at postmidnight, not the auroral bulge at premidnight.

4. Discussion

[24] We have obtained that the occurrence rates of the earthward fast flows are decreasing as Geotail moves closer to the Earth at $X < -15\ R_E$. This result can be interpreted by the braking of the earthward fast flows [*Shiokawa et al.*, 1997]. The earthward fast flows observed at $-15 > X > -30\ R_E$ can be related to various generation mechanisms such as the near-Earth magnetic reconnection [*Hones*, 1976], the mid-tail current disruption [*Lui et al.*, 1991], polarization electric fields [*Chen and Wolf*, 1993], the magnetic reconnection in the distant tail [*Nagai and Machida*, 1998], a retreat of tailward fast flows [*Baumjohann et al.*, 1999], and enhancements of large-scale ULF oscillations [*Lyons et al.*, 2002]. As the plasma flows move closer to the Earth, the flow speed will slow down due to the stronger magnetic pressure near the Earth [*Shiokawa et al.*, 1997]. A recent study by *Ohtani et al.* [2006] concluded that most of fast flows do not affect anything around the

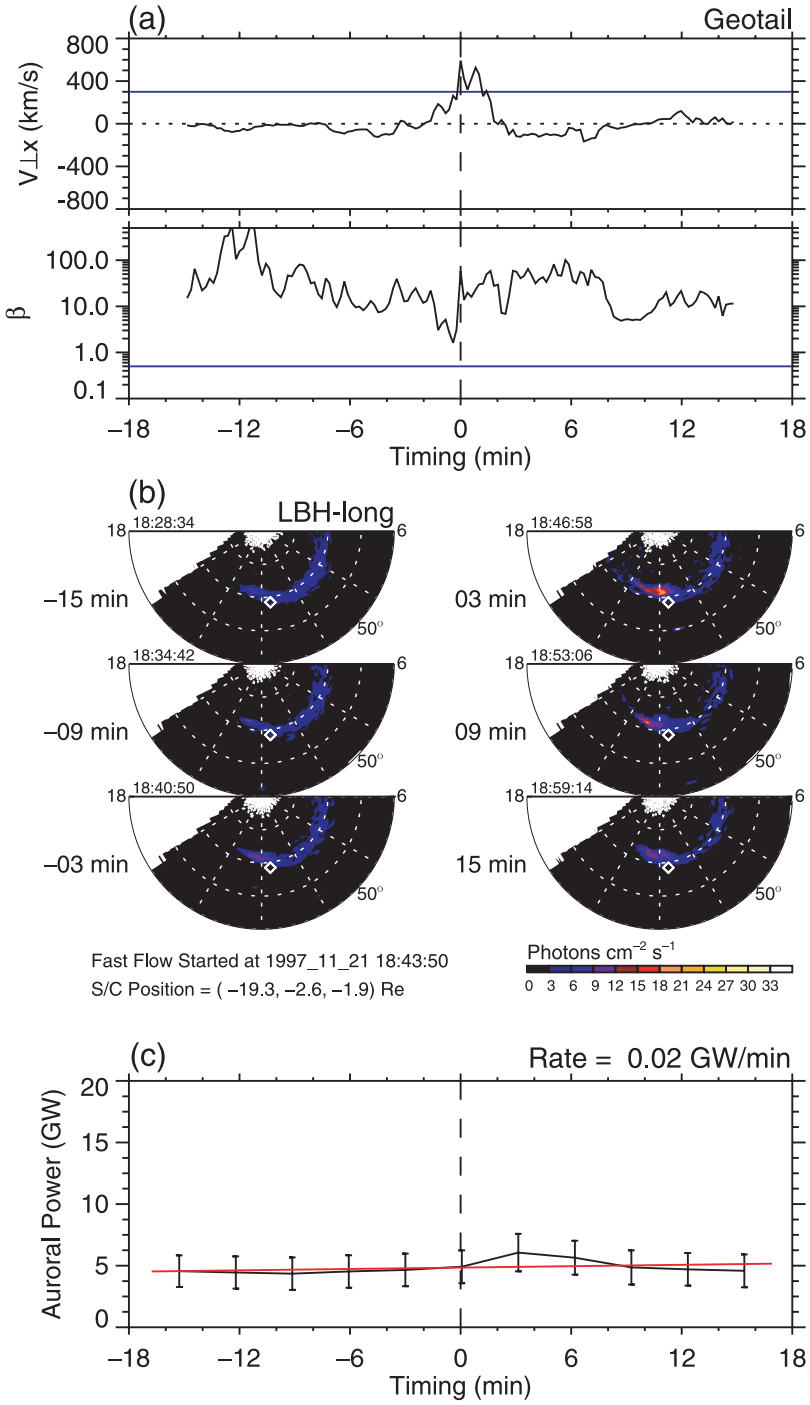

Figure 5. Observations of Geotail plasma and magnetic fields and Polar Ultraviolet Imager (UVI) auroral images for the 21 November 1997 event. The format is the same as that for Figure 1.

geosynchronous orbit. Interestingly, in Figure 3, the occurrence rate for $X = -10\ R_E$ is almost the same as that for $X = -15\ R_E$. This result can be interpreted as that a current disruption occurred near $X = \sim -10\ R_E$ can cause a force imbalance which results in an acceleration of the plasma to a fast speed [*Lui et al.*, 1993].

[25] Figure 3 shows that the occurrence rates of the earthward fast flows are, in general, decreasing as Geotail comes closer to the Earth, implying that it is difficult for the fast flows to propagate to $X = \sim -10\ R_E$ when one is created at $X = \sim -30\ R_E$. The earthward fast flows observed at $X = \sim -10\ R_E$ are likely related to the local mechanism. The current disruption mechanism is a candidate to create the earthward fast flows. Either the braking of the earthward fast flows generated at $X < -15\ R_E$ or some instabilities can trigger the current disruption. The current disruption can subsequently generate an earthward fast flow at $X = \sim -10\ R_E$.

[26] All the earthward fast flows in Class *I* are related to a high auroral power rate of change in terms of time. The corresponding auroral images to the events indicate that

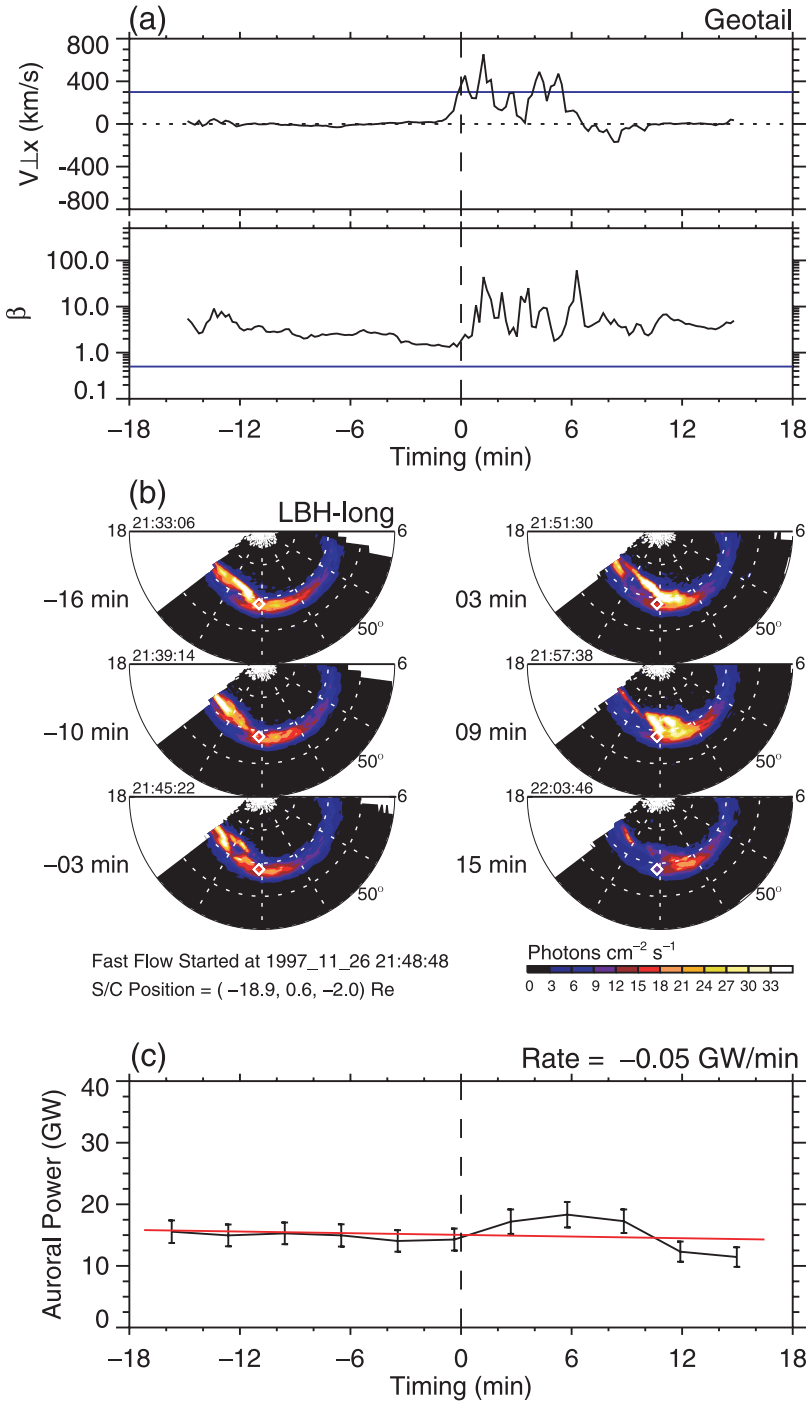

Figure 6. Observations of Geotail plasma and magnetic fields and Polar Ultraviolet Imager (UVI) auroral images for the 26 November 1997 event. The format is the same as that for Figure 1.

there was an auroral bulge developed on the nightside, an indicator of a substorm. This result is consistent with the result by *Angelopoulos et al.* [1999] who found that the current disruption and fast flows are qualitatively similar phenomena in the near-Earth tail ($X = \sim -10\ R_E$). Both phenomena are associated with the occurrence of a substorm. Thus this class of earthward fast flows plays an important role in the global auroral development.

[27] Most of the earthward fast flows in Class *II* are related to a low auroral power rate of change. The associated auroral features are pseudobreakups or PBIs, which is consistent with the results by *Nakamura et al.* [2001]. They have concluded that all the earthward fast flows in their data set correspond to the localized auroral activations. Our events shown in Figures 5 and 6 are consistent with their results. Note that their data set did not include the events of large substorms. All these results imply that most of the

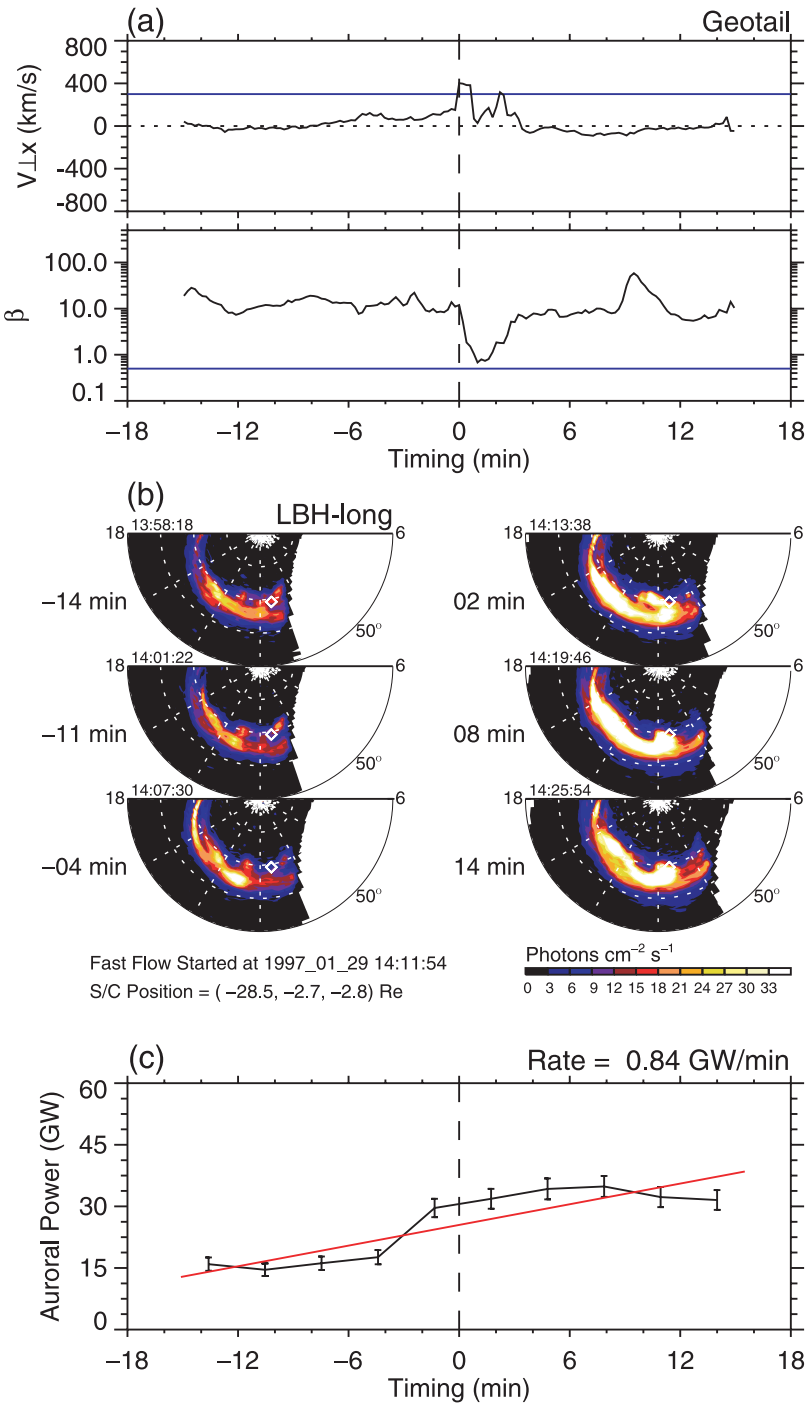

Figure 7. Observations of Geotail plasma and magnetic fields and Polar Ultraviolet Imager (UVI) auroral images for the 29 January 1997 event. The format is the same as that for Figure 1.

earthward fast flows in Class *II* do not play an important role in the global auroral development.

[28] There are still a few earthward fast flow events in Class *II* associated with high auroral power rates of change, which indicates an auroral bulge developed on the nightside and the current disruption occurred at $X = \sim -10\ R_E$. We suspect that the earthward fast flows observed at $X < -15\ R_E$ are not directly related to the auroral bulge. If we had simultaneous observations near $X = \sim -10\ R_E$ for these events, we would observe an earthward fast flow for the auroral bulge. Unfortunately, we currently do not have such simultaneous observations to verify this speculation. Our hypothesis is that the earthward fast flows in Class *II* create only the localized auroral activations. An auroral bulge may coincidently occur with the earthward fast flow observed at $X < -15\ R_E$, which results in the high auroral power rate for the event. We plan to examine the existence of an earthward fast flow at $X = \sim -10\ R_E$ when an auroral bulge is found on the nightside by using the ground-based images and multiple satellite data from the THEMIS mission in the future.

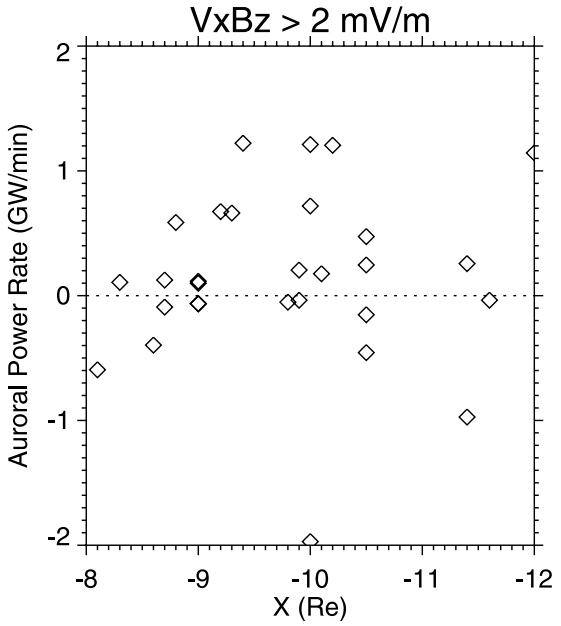

Figure 8. Auroral power rates of change estimated over the courses of earthward flows with rapid flux transport (V_xB_z > 2 mV/m) in terms of X in the GSM coordinate system. The auroral power is integrated over a region of 60–80° MLAT and 2000–0400 MLT.

[29] Whether or not the earthward fast flows in Class *II* play an important role in the global auroral activation depends upon how we view the problem. If we consider a fast flow itself on the way to $X = \sim -10\ R_E$, the direct consequence of a fast flow is the localized auroral activation [*Nakamura et al.*, 2001]. This fast flow, therefore, does not play an important role in the global auroral activation. If we consider a substorm triggered by the braking of the fast flow [*Shiokawa et al.*, 1997], the indirect consequence of the fast flow is the global auroral activation. Note that the strength of a substorm auroral bulge is much more intense than a localized auroral activation. When the substorm is developing, the development of the localized activation will not be clearly seen unless the two types of the auroral activations are separated at a large distance, like the event shown in Figure 7.

[30] It should be noted that we derive the auroral power rates of change over the courses of earthward fast flows for our study. The auroral power can be used to evaluate the large-scale impact of the localized fast flows in terms of the auroral energy into the high-latitude ionosphere. The auroral power may increase slightly in response to a localized auroral activation related to a fast flow, see the events shown in Figures 5 and 6.

[31] The magnetotail is commonly highly structured and time-varying. Simulations [e.g., *Shay et al.*, 2003] show a large variety of fast flows occurring in different locations at the same time. Since we have limited observations in the tail, we cannot observe every one of the fast flows. With the limited number of the flows observed by Geotail, it is often difficult to tell whether the fast flows are associated with the local or global auroral activations. We have found several events (Class *II*) in which a full-developed substorm appears after the occurrence of the fast plasma flows. The fast flows may establish a favorable condition for the current disruption process to proceed, and therefore the substorm may develop following the generation of the fast flows [*Ohtani et al.*, 2002].

[32] Six events in Class *I* ($-8 > X > -12\ R_E$) may be insufficient for a quantitative evaluation. However, all these events show a consistent feature of high auroral power rates of change. We have tried to add more events for Class *I* by relaxing our criterion of "nine or more images" to "three or more images" for event selection. This relaxation has enabled us to find two more events. From examining the Polar UVI images for the two events, an auroral bulge on the nightside was observed. The resulting auroral power rates of change are 5.01 and 1.00 GW/min, respectively. Since the number of the images used for the calculation of the power rates of change for the two events is only four, the significance of the fitting is low. Thus we do not add them to the scatter points in Figure 4. One thing we want to emphasize is that the feature shown from the two events is consistent with our conclusion for the fast flow events in Class *I*: the auroral power rate of change is always high in this class.

[33] We have also used another criterion of event selection which is similar to that used by *Schödel et al.* [2001] ($\beta > 0.5$, $V_x > 0$, $V_{\perp x} > V_{\|x}$, and $V_xB_z > 2$ mV/m) to find earthward flow events with rapid flux transport (RFT) at a region of $-8 > X > -12\ R_E$ and $|Y| < 6\ R_E$ for Class *I*, where B_z is the Z component of the magnetic field, $V_{\|}x$ is the X component of the plasma flow parallel to the ambient magnetic field, and V_xB_z is the convection electric field. We have found 29 RFT events from this selection criterion. The auroral power rates of change in terms of time have been estimated for these RFT events by using the least squares method. These auroral power rates of change are plotted against X, as shown in Figure 8. It is found that the auroral power rates for most of the RFT events are small, but a few of them are high, which is similar to the feature for Class *II*. If the criterion of V_xB_z is used in the identification of the events, we are unable to distinguish the two classes of the plasma sheet fast flows. It indicates that $V_{\perp x}$ is a better parameter than V_xB_z to differentiate the class of earthward fast flows in the plasma sheet.

[34] One may argue that the results of Figure 8 indicate that the fast flows at $X = \sim -10\ R_E$ selected by the flux transport criteria do not necessarily accompany with the auroral bulge, which is inconsistent with the main point for the events selected by the velocity criteria: all the fast flows in Class *I* are associated with the auroral bulge. This argument is raised based on an assumption of that the fast flows selected by the flux transport criteria and the velocity criteria are the same phenomena. However, our preliminary comparison between the two types of criteria indicates that they are not the same. To further support this result, we examine the maximum $V_{\perp x}$ for the RFT events with lower auroral activations by using the criteria of "rate of change <0.3 GW/min" and "the average auroral power for a period of 15 minutes before the starting time of the RFTs <30 GW." We have found 12 events that fit the criteria. The values of the maximum $V_{\perp}x$ for these selected events varies from 66 to 247 km/s. Since all the values of the maximum $V_{\perp x}$ are less 300 km/s, we believe that our criterion value of the fast

flows ($V_{\perp x}$ < 300 km/s) is reasonable to differentiate the class of earthward fast flows in the plasma sheet.

5. Summary

[35] We have examined 68 earthward fast flows observed at $|Y| < 6\ R_E$ with the simultaneous observations of Polar UVI auroral images. It is found that the earthward fast flows can be classified into two classes. One class of the fast flows (Class *I*) was often observed near $X = \sim -10\ R_E$ and the other class (Class *II*) was found at $X < -15\ R_E$. The auroral power rates for the fast flows in Class *I* are found to be high, indicating the auroral brightness on the nightside was significantly increasing over the courses of these fast flows. The auroral images show an apparent substorm auroral bulge developed on the nightside. The auroral power rates for most of the fast flows in Class *II* are low. The auroral features, such as poleward boundary intensifications and pseudobreakups, are found to be associated with the fast flows in Class *II*. We hypothesize that the direct consequence of the earthward fast flows observed at $X < -15\ R_E$ is a localized auroral activation. A substorm may occur at $X = \sim -10\ R_E$ due to the braking of the fast flows or some instability. A current disruption related to the substorm may generate an earthward fast flow at $X = \sim -10\ R_E$. Since the occurrence rates of the earthward fast flows are decreasing as Geotail comes closer to the Earth due to the stronger magnetic field intensity near Earth, keeping relatively constant occurrence rate at $X = -10\ R_E$ and $X = -15\ R_E$ is most likely contributed by the fast flows generated by the current disruption. The hypothesis will be tested with the multiple satellite data from the THEMIS mission in the future.

[36] **Acknowledgments.** This work was supported in part by National Space Organization grant 95-NSPO(B)-SP-FA07-01 and National Science Council grant NSC 95-2111-M-008-019 to National Central University and in part by Ministry of Education under the Aim for Top University program at NCU. Geotail data were provided from the Data Archives and Transmission System (DARTS) of Institute of Space and Astronautical Science (ISAS).

[37] Wolfgang Baumjohann thanks Kazuo Shiokawa and another reviewer for their assistance in evaluating this paper.

References

Akasofu, S.-I. (1964), The development of auroral substorm, *Planet. Space Sci.*, *12*, 273–282.

Angelopoulos, V., W. Baumjohann, C. F. Kennel, F. V. Coroniti, M. G. Kivelson, R. Pellat, R. J. Walker, and G. Paschmann (1992), Bursty bulk flows in the inner central plasma sheet, *J. Geophys. Res.*, *97*, 4027–4039.

Angelopoulos, V., C. F. Kennel, F. V. Coroniti, R. Pellat, M. G. Kivelson, R. J. Walker, C. T. Russell, W. Baumjohann, W. C. Feldman, and J. T. Gosling (1994), Statistical characteristics of bursty bulk flow events, *J. Geophys. Res.*, *99*, 21,257–21,280.

Angelopoulos, V., T. D. Phan, D. E. Larson, et al. (1997), Magnetotail flow bursts: association to global magnetospheric circulation, relationship to ionospheric activity and direct evidence for localization, *Geophys. Res. Lett.*, *24*, 2271–2274.

Angelopoulos, V., F. S. Mozer, T. Mukai, K. Tsuruda, S. Kokubun, and T. J. Hughes (1999), On the relationship between bursty flows, current disruption and substorms, *Geophys. Res. Lett.*, *26*, 2841–2844.

Baumjohann, W., G. Paschmann, N. Sckopke, C. A. Cattell, and C. W. Carlson (1988), Average ion moments in the plasma sheet boundary layer, *J. Geophys. Res.*, *93*, 11,507–11,520.

Baumjohann, W., G. Paschmann, and C. A. Cattell (1989), Average plasma properties in the central plasma sheet, *J. Geophys. Res.*, *94*, 6597–6606.

Baumjohann, W., G. Paschmann, and H. Lühr (1990), Characteristics of high-speed ion flows in the plasma sheet, *J. Geophys. Res.*, *95*, 3801–3809.

Baumjohann, W., M. Hesse, S. Kokubun, T. Mukai, T. Nagai, and A. A. Petrukovich (1999), Substorm dipolarization and recovery, *J. Geophys. Res.*, *104*, 24,995–25,000.

Birn, J., and M. Hesse (1996), Details of current disruption and diversion in simulations of magnetotail dynamics, *J. Geophys. Res.*, *101*, 15,345–15,358.

Chen, C. X., and R. A. Wolf (1993), Interpretation of high-speed flows in the plasma sheet, *J. Geophys. Res.*, *98*, 21,409–21,420.

Fairfield, D. H., T. Mukai, Y. Yamamoto, et al. (1999), Earthward flow bursts in the inner magnetotail and their relation to auroral brightenings, AKR intensifications, geosynchronous particle injections and magnetic activity, *J. Geophys. Res.*, *104*, 355–370.

Hones, E. W., Jr. (1976), The magnetotail: Its generation and dissipation, in *Physics of Solar Planetary Environments*, edited by D. J. Williams, pp. 558–571, AGU, Washington, D. C.

Huang, C. Y., and L. A. Frank (1986), A statistical study of the central plasma sheet: Implications for substorm models, *Geophys. Res. Lett.*, *13*, 652–655.

Ieda, A., J.-H. Shue, K. Liou, et al. (2003), Quiet time magnetotail plasma flow: Coordinated Polar ultraviolet images and Geotail observations, *J. Geophys. Res.*, *108*(A9), 1345, doi:10.1029/2002JA009739.

Kokubun, S., T. Yamamoto, M. H. Acuña, K. Hayashi, K. Shiokawa, and H. Kawano (1994), The GEOTAIL magnetic field experiment, *J. Geomagn. Geoelectr.*, *46*, 7–21.

Lui, A. T. Y., C.-L. Chang, A. Mankofsky, H.-K. Wong, and D. Winske (1991), A cross-field current instability for substorm expansions, *J. Geophys. Res.*, *96*, 11,389–11,401.

Lui, A. T. Y., P. H. Yoon, and C. L. Chang (1993), Quasi-linear analysis of ion Weibel instability, *J. Geophys. Res.*, *98*, 153–164.

Lui, A. T. Y., K. Liou, P. T. Newell, C.-I. Meng, S.-I. Ohtani, T. Ogino, S. Kokubun, M. J. Brittnacher, and G. K. Parks (1998), Plasma and magnetic flux transport associated with auroral breakups, *Geophys. Res. Lett.*, *25*, 4059–4062.

Lui, A. T. Y., K. Liou, M. Nosé, S. Ohtani, D. J. Williams, T. Mukai, K. Tsuruda, and S. Kokubun (1999), Near-Earth dipolarization: Evidence for a non-MHD process, *Geophys. Res. Lett.*, *26*, 2905–2908.

Lyons, L. R., T. Nagai, G. T. Blanchard, J. C. Samson, T. Yamamoto, T. Mukai, A. Nishida, and S. Kokubun (1999), Association between Geotail plasma flows and auroral poleward boundary intensifications observed by CANOPUS photometers, *J. Geophys. Res.*, *104*, 4485–4500.

Lyons, L. R., E. Zesta, Y. Xu, E. R. Sánchez, J. C. Samson, G. D. Reeves, J. M. Ruohoniemi, and J. B. Sigwarth (2002), Auroral poleward boundary intensifications and tail bursty flows: A manifestation of a large-scale ULF oscillation, *J. Geophys. Res.*, *107*(A11), 1352, doi:10.1029/2001JA000242.

Machida, S., Y. Miyashita, A. Ieda, A. Nishida, T. Mukai, Y. Saito, and S. Kokubun (1999), GEOTAIL observations of flow velocity and north-south magnetic field variations in the near and mid-distant tail associated with substorm onsets, *Geophys. Res. Lett.*, *26*(6), 635–638.

Miyashita, Y., S. Machida, K. Liou, T. Mukai, Y. Saito, H. Hayakawa, C.-I. Meng, and G. K. Parks (2003), Evolution of the magnetotail associated with substorm auroral breakups, *J. Geophys. Res.*, *108*(A9), 1353, doi:10.1029/2003JA009939.

Mukai, T., S. Machida, Y. Saito, M. Hirahara, T. Terasawa, N. Kaya, T. Obara, M. Ejiri, and A. Nishida (1994), The low-energy particle (LEP) experiment onboard the Geotail satellite, *J. Geomagn. Geoelectr.*, *46*, 669–692.

Nagai, T., and S. Machida (1998), Magnetic reconnection in the near-Earth magnetotail, in *New Perspectives on the Earth's Magnetotail*, *Geophys. Monogr. Ser.*, vol. 105, edited by A. Nishida, D. N. Baker, and S. W. H. Cowley, pp. 211–224, AGU, Washington D. C.

Nagai, T., M. Fujimoto, Y. Saito, S. Machida, T. Terasawa, R. Nakamura, T. Yamamoto, T. Mukai, A. Nishida, and S. Kokubun (1998), Structure and dynamics of magnetic reconnection for substorm onsets with Geotail observations, *J. Geophys. Res.*, *103*(A3), 4419–4440.

Nakamura, R., W. Baumjohann, M. Brittnacher, V. A. Sergeev, M. Kubyshkina, T. Mukai, and K. Liou (2001), Flow bursts and auroral activations: Onset timing and foot point location, *J. Geophys. Res.*, *106*(A6), 10,777–10,790.

Ohtani, S., R. Yamaguchi, M. Nosé, H. Kawano, M. Engebretson, and K. Yumoto (2002), Quiet time magnetotail dynamics and their implications for the substorm trigger, *J. Geophys. Res.*, *107*(A2), 1030, doi:10.1029/2001JA000116.

Ohtani, S., M. A. Shay, and T. Mukai (2004), Temporal structure of the fast convective flow in the plasma sheet: Comparison between observations and two-fluid simulations, *J. Geophys. Res.*, *109*, A03210, doi:10.1029/2003JA010002.

Ohtani, S., H. J. Singer, and T. Mukai (2006), Effects of the fast plasma sheet flow on the geosynchronous magnetic configuration: Geotail and GOES coordinated study, *J. Geophys. Res.*, *111*, A01204, doi:10.1029/2005JA011383.

Paterson, W. R., L. A. Frank, S. Kokubun, and T. Yamamoto (1998), Geotail survey of ion flow in the plasma sheet: Observations between 10 and 50 R_E, *J. Geophys. Res.*, *103*, 11,811–11,826.

Schödel, R., W. Baumjohann, R. Nakamura, V. A. Sergeev, and T. Mukai (2001), Rapid flux transport in the central plasma sheet, *J. Geophys. Res.*, *106*, 301–314.

Shay, M. A., J. F. Drake, M. Swisdak, W. Dorland, and B. N. Rogers (2003), Inherently three dimensional magnetic reconnection: A mechanism for bursty bulk flows?, *Geophys. Res. Lett.*, *30*(6), 1345, doi:10.1029/2002GL016267.

Shiokawa, K., W. Baumjohann, and G. Haerendel (1997), Braking of high-speed flows in the near-Earth tail, *Geophys. Res. Lett.*, *24*(10), 1179–1182.

Shue, J.-H., S. Ohtani, P. T. Newell, K. Liou, C.-I. Meng, A. Ieda, and T. Mukai (2003), Quantitative relationships between plasma sheet fast flows and nightside auroral power, *J. Geophys. Res.*, *108*(A6), 1231, doi:10.1029/2002JA009794.

Slavin, J. A., D. H. Fairfield, R. P. Lepping, et al. (1997), WIND, GEOTAIL, and GOES 9 observations of magnetic field dipolarization and bursty bulk flows in the near-tail, *Geophys. Res. Lett.*, *24*, 971–974.

Torr, M. R., D. G. Torr, M. Zukic, et al. (1995), A far ultraviolet imager for the International Solar-Terrestrial Physics mission, *Space Sci. Rev.*, *71*, 329–383.

Tsyganenko, N. A. (1989), A magnetospheric magnetic field model with a warped tail current sheet, *Planet. Space Sci.*, *37*, 5–20.

A. Ieda, Solar-Terrestrial Environment Laboratory, Nagoya University, Nagoya, Aichi, 464-8601, Japan. (ieda@stelab.nagoya-u.ac.jp)

A. T. Y. Lui and S. Ohtani, Applied Physics Laboratory, Johns Hopkins University, 11100 Johns Hopkins Road, Laurel, MD 20723-6099, USA. (tony.lui@jhuapl.edu; shin.ohtani@jhuapl.edu)

T. Mukai, Institute of Space and Astronautical Science, Japan Aerospace Exploration Agency, 3-1-1 Yoshinodai, Sagamihara, Kanagawa, 229-8510, Japan. (mukai@stp.isas.jaxa.jp)

G. K. Parks, Space Sciences Laboratory, University of California, Berkeley, CA 94720, USA. (parks@ssl.berkeley.edu)

J.-H. Shue, Institute of Space Science and Department of Atmospheric Sciences, National Central University, Jhongli City, Taoyuan County, 32001, Taiwan. (jhshue@jupiter.ss.ncu.edu.tw)